Propagation velocity of Alfvén wave packets in a dissipative plasma

Yoshimitsu Amagishi and Hiroyuki Nakagawa
Faculty of Liberal Arts, Shizuoka University, 836 Ohya, Shizuoka 422, Japan

Masayoshi Tanaka
Department of High Energy Engineering Science, Interdisciplinary Graduate School of Engineering Science, Kyushu University, Kasuga, Fukuoka 816, Japan

(Received 5 April 1994)

We have experimentally studied the behavior of Alfvén wave packets in a dissipative plasma due to ion–neutral-atom collisions. It is urged that the central frequency of the packet is observed to gradually decrease with traveling distance in the absorption range of frequencies because of a differential damping among the Fourier components, and that the measured average velocity of its peak amplitude is not accounted for by the conventional group velocity, but by the prediction derived by Tanaka, Fujiwara, and Ikegami [Phys. Rev. A **34**, 4851 (1986)]. Furthermore, when the initial central frequency is close to the critical frequency in the anomalous dispersion, the wave packet apparently collapses when traveling along the magnetic field; however, we have found that it is decomposed into another two wave packets with the central frequencies being higher or lower than the critical frequency.

PACS number(s): 52.40.Db, 03.40.Kf

I. INTRODUCTION

A localized absorption in a dispersive medium generally produces a negative slope on the dispersion curve (anomalous dispersion) in a certain frequency range, because the real and imaginary parts of the dielectric function are related to each other by the causality principle, i.e., the Kramers-Kronig relation. In such a region of the anomalous dispersion, the group velocity defined by

$$v_g = \frac{c}{\mathrm{Re}\left(\frac{\partial n\omega}{\partial \omega}\right)_{\omega_c}}, \tag{1}$$

where c is the light velocity, n the complex refractive index, and ω_c the initial central frequency of the wave packet, exceeds the light velocity or even becomes negative. A number of theories [1–5] have hitherto been proposed to have a clear physical interpretation of the group velocity. Recently, it has been clarified in Refs. [6,7] that the average velocity of a Gaussian wave packet, defined as the traveling distance z of the peak amplitude of the wave packet divided by its flight time t, is given, by means of the saddle-point method, as follows:

$$\frac{z}{t} = \frac{c}{\mathrm{Re}\left(\frac{\partial n\omega}{\partial \omega}\right)_{\omega_1}}. \tag{2}$$

Here we should note that the derivative is taken at a saddle-point frequency ω_1, which is a real number for the peak amplitude of the packet and is obtained from the following relation (see Appendix A),

$$\omega_1 - \omega_c = -\frac{z}{c\Delta^2}\mathrm{Im}\left(\frac{\partial n\omega}{\partial \omega}\right)_{\omega_1}, \tag{3}$$

where Δ is the pulse width of the initial wave packet. The velocity given by Eq. (2) includes the effects of both packet deformation and spreading, and coincides with the group velocity Eq. (1) when absorption is negligible, but it remarkably deviates from the group velocity for strong absorption. Equation (3) indicates that the frequency ω_1, which corresponds to the central frequency of the packet, slowly changes along the traveling distance because of a differential damping among the Fourier components. In other words, the Fourier components closer to the critical frequency, at which the group velocity defined by Eq. (1) takes the value of infinity, attenuate faster than the rest, and the resultant central frequency of the spectrum shifts toward the nonresonant region. Another work [8], which appears later, has obtained the same results by treating the problem as an initial value one.

In a preliminary experiment [9], we have found that an anomalous dispersion relation of the shear Alfvén wave appears on the complex refractive index curve owing to ion-neutral collisions and that a wave packet in this frequency range undergoes strong amplitude damping and profile deformation. We have also confirmed that the Kramers-Kronig relation holds for the dielectric function of the Alfvén wave in the absorption region. We will conclude, in this paper, that the peak velocity of the shear-Alfvén-wave packet discussed in our previous paper does not obey the conventional group velocity given by Eq. (1) in the absorption range of frequency but the alternative velocity defined by Eq. (2).

II. EXPERIMENTAL PROCEDURE

The experiment was performed in the linear device TPH (test plasma of high density) of Shizuoka University (15 cm diam, 3 m length) as shown in Fig. 1, in which a quasisteady (2 ms) current-free, high-density ($\lesssim 5 \times 10^{21}$ m^{-3}) streaming and singly ionized helium plasma was established by a pulsed magneto-plasma-dynamic (MPD) arcjet with an anode hole of 4 cm diameter. Fundamental experiments on the Alfvén wave and MHD surface wave have been carried out by using the TPH for more than a decade (see, for example, Refs. [10–13]).

To carry out the present experiment, we chose for typical pulsed parameters the plasma density 4×10^{20} m^{-3} at the center, an ion temperature $T_i \lesssim 20$ eV, and an electron temperature $T_e \sim 5$ eV at the center, and spatially uniform magnetic field $B_0 = 0.3$ T, which gives an ion-cyclotron frequency $\omega_{ci} = 7.2 \times 10^6$ rad/s. As we have concluded in Ref. [9], the ionization rate was about 60% for this experiment. Then the strong absorption range of frequency should be localized around the critical frequency $\omega^* = (4.5\text{–}5) \times 10^6$ rad/s as has been discussed in Ref. [9].

We designed a small antenna for the experiment described in Ref. [9] in order to directly excite the shear Alfvén wave of the poloidal wave number $m = 0$ near the plasma center. Antenna excitation was achieved by discharging capacitors charged up to ~ 10 kV, which were connected to the antenna in a series. Although the form of an antenna current is a damped sinusoidal oscillation, the wave pulse in the plasma is immediately reshaped to a packet like a Gaussian type, owing to the dispersion of the plasma.

In addition to two usual magnetic probes inserted radially, another small magnetic probe movable along the magnetic field B_0 (z direction) at $r = 1$ cm, was provided to measure more precisely both attenuation constants and distortion of the wave packet as it travels along the z direction. Time-dependent data was averaged at least in five shots of discharge per position to calculate auto- and cross-power-spectral densities of the propagating wave packets. The raw data was processed digitally by using a data acquisition system (see Ref. [10]).

III. EXPERIMENTAL RESULTS AND DISCUSSIONS

The complex refractive index $n = n_r + in_i$ in the z direction was experimentally obtained (Fig. 2); the real part n_r is the same one given in Ref. [9], but the imaginary part n_i was calculated from more precise attenuation constants of the packets in the z direction that were obtained by using the movable magnetic probe. Solid lines in both figures represent the curve best fit for the data as will be mentioned below.

Let us see examples of spatial evolution of the magnetic component b_θ of the wave packet, propagating along the z direction at $r = 1$ cm. Figure 3 shows that the wave packet propagates through an absorbing medium with a decrease in its central frequency, and that its packet

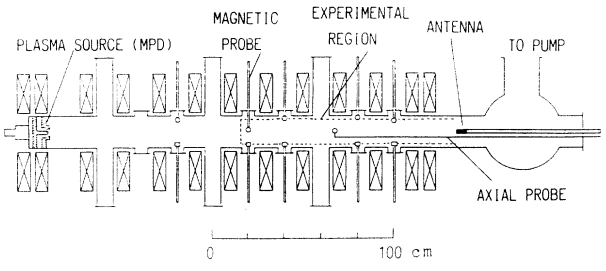

FIG. 1. Schematic view of the experimental device TPH.

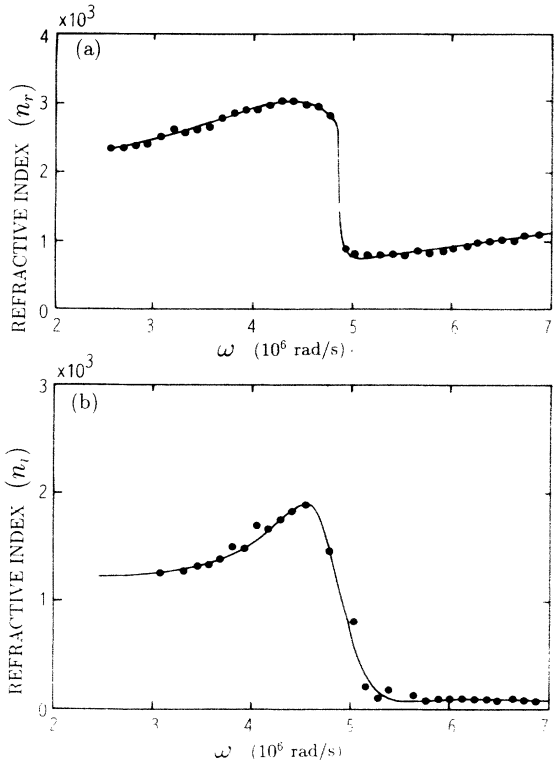

FIG. 2. Complex refractive index calculated from evolution of the launched waves along the z direction. (a) Real part. (b) Imaginary part.

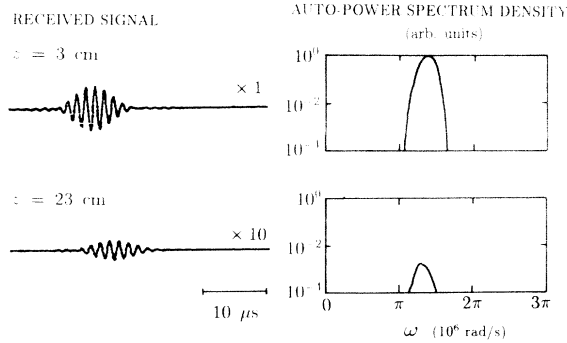

FIG. 3. Observed wave packets and autopower spectra of the magnetic field b_θ of shear Alfvén waves. $\omega_c = 4.33 \times 10^6$ rad/s.

profile looks self-similar but is changing its amplitude. The dispersion relation of this mode has been identified [9] as that of the shear Alfvén wave including ion-neutral collisions, which is given by

$$S\frac{\omega^2}{k_\parallel^2 V_A^2} - \left(1 - S^2\frac{\omega^2}{\omega_{ci}^2}\right) = 0, \tag{4}$$

with the complex factor S given by

$$S = 1 + \frac{\frac{\rho_n}{\rho_0}}{1 - i\frac{\rho_n}{\rho_0}\frac{\omega}{\nu_{in}}}, \tag{5}$$

where ρ_0 and ρ_n are, respectively, the mass density of the ion and neutral, and ν_{in} the ion-neutral collision frequency.

Figure 4, on the other hand, shows the wave packet of the compressional Alfvén wave whose initial central frequency is higher than the critical frequency ω^*. This mode has been identified [9] as the $m = +1$ first radial eigenmode of the fast wave, whose dispersion relation is, not like the shear-Alfvén continuous spectrum, determined by the density and electric resistivity profiles, and boundary conditions in the radial direction, as discussed in Ref. [12]. In this case, the central frequency does not shift within experimental errors because the compressional Alfvén wave in this range of frequency is little subject to the ion-neutral collision.

Figure 5 demonstrates that the measured central frequency of the shear-Alfvén-wave packet is a function of traveling distance. The solid line in Fig. 5 indicates a theoretical value calculated from Eq. (3). In order to solve Eq. (3), we first fit a linear combination of analytic functions to the experimental data of $n_i(\omega)$ shown in Fig. 2(b), and then differentiating the fitting function and substituting the differential values in to Eq. (3), we search numerical solutions for ω_1 (those procedures are easily followed by means of Mathematica). Figure 5 clearly shows that close agreement has been obtained between the experimental shift of the central frequency and the theoretical one: the conventional group velocity given by Eq. (1) is based on the assumption that the central

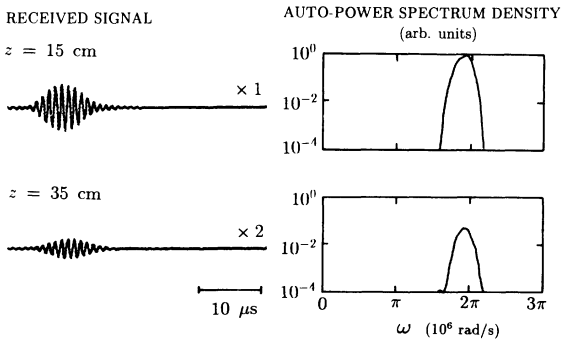

FIG. 4. Observed wave packets and autopower spectra of the magnetic field b_θ of compressional Alfvén waves. $\omega_c = 5.88 \times 10^6$ rad/s.

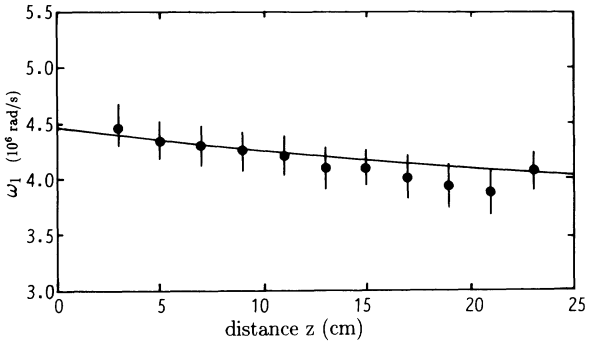

FIG. 5. An example of central frequency ω_1 shifting along the traveling distance z. The closed circle indicates the experimental values, and the vertical bar does a half peak width at half height of the autopower spectrum. The solid line is the result calculated from Eq. (3) by putting $\Delta = 3.6$ μs and the central frequency of the antenna current $\omega_c = 4.48\times10^6$ rad/s.

frequency remains unchanged and is equal to the initial one, but it does change as has been predicted by the theory [6,7].

We next estimate average velocities of the packet in the z direction, from the time difference between two peak amplitudes of the wave packets received through two probes at intervals of 20 cm: a spline interpolation was applied to the received signals to calculate the wave envelope. The measured velocity of the wave packet is shown in Fig. 6 as a function of the initial central frequency ω_c. The solid curve in this figure represents the velocity calculated from Eq. (2) with Eq. (3). In a medium with moderate absorption, it is experimentally hard to distinguish between two velocities, i.e., Eqs. (1) and (2), but for the initial central frequencies in the neighborhood of the anomalous dispersion of the shear Alfvén wave, the

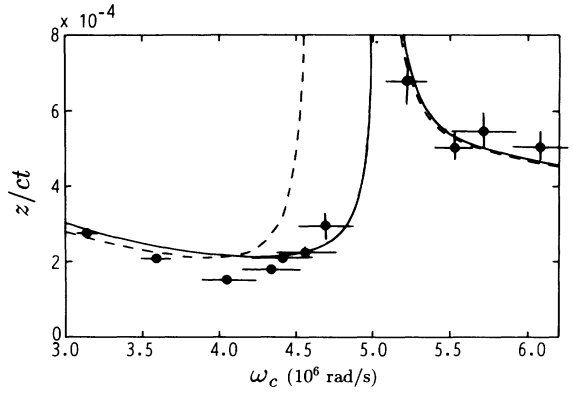

FIG. 6. Comparison of the measured velocities of the packets with the calculated velocities. The horizontal bar indicates a half peak width at half height of the autopower spectrum, while the vertical bar does measurement errors. The solid line represents the velocity calculated from Eq. (2) with Eq. (3) by putting $\Delta = 3.6$ μs and traveling distance 20 cm. The dash line represents the conventional group velocity calculated from Eq. (1).

measured velocities never go towards infinity as the conventional group velocity shown in Fig. 6 by the dash line, but follow the velocity given by Eq. (2).

It is further of interest to know how the wave packet behaves when the initial central frequency $\omega \sim \omega^*$ and the Fourier spectrum includes the components of not only the shear Alfvén wave but also the compressional wave. In this case the wave packet, as shown in Fig. 7(a), is strongly decayed and deformed as leaving from the antenna; the group velocity then cannot be defined anymore from the original wave form. By passing through digital high- and low-pass filters, however, the wave packet is observed to consist of another two wave packets, from which the velocity of each packet can be estimated again. The auto-power-spectral density and its coherency for the data corresponding to Figs. 7(a) are shown, respectively, in Figs. 7(b) and 7(c), where we can see that the amplitude at the frequency $\sim \omega^*$ is rapidly decreased and hence the coherency around ω^* becomes worse as the traveling distance increases, while another two peaks appear with the central frequencies higher or lower than the critical frequency ω^*.

In conclusion, our experiment supports the alternative

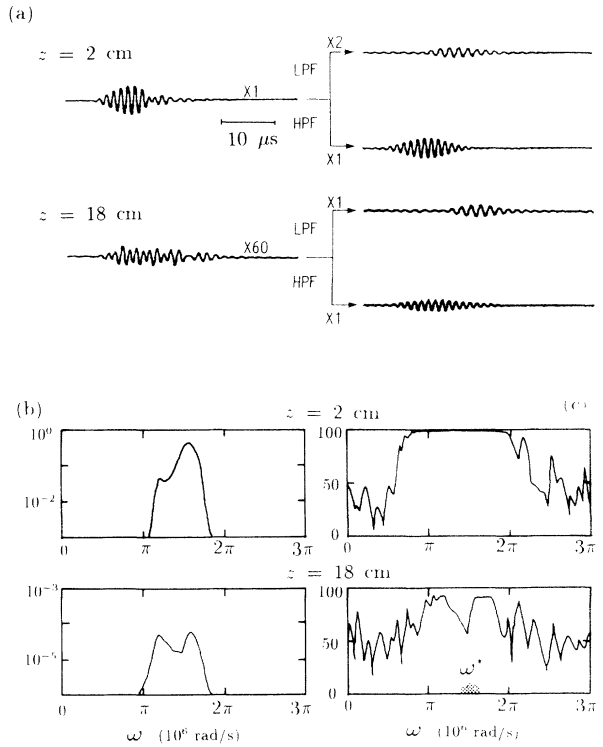

FIG. 7. Deformation and split of the packet composed of the shear and compressional Alfvén waves with the initial central frequency $\omega \sim \omega^*$. (a) Wave packets received at $z = 2$ and 18 cm, which are decomposed into high and low frequency components by passing through digital filters. (b) Auto-power-spectral density (arb. units) of the magnetic field b_θ for wave packets shown in (a). (c) Coherency (%), which is defined by the absolute value of cross-power-spectral density between received signal and antenna current, divided by the square root of respective auto-power-spectral densities.

"group velocity" defined by Eq. (2) with Eq. (3). Concerning the behavior of wave packets in dissipative media, it is crucial that the wave packet is characterized by a shifting its central frequency as it propagates even in a homogeneous medium. In regard to the split of wave packets when the initial central frequency $\omega \sim \omega^*$, we may say that it is explained essentially by Eq. (A3) for a small value of Δ and a specific refractive index, but since theoretical considerations of the split are beyond this paper, we will discuss it in detail in a further publication.

ACKNOWLEDGMENT

This work was supported in part by a Grant-in-Aid for Science Research from the Ministry of Education, Science, and Culture of Japan.

APPENDIX A

We briefly summarize the saddle-point method which we have applied to the wave packet propagation. A wave packet propagating in dispersive media is expressed by the following Fourier integral:

$$\phi(z,t) = \frac{1}{\sqrt{2\pi}} \int_{-\infty}^{\infty} d\omega \exp\left[\frac{z}{z_0} P(\omega)\right] + \text{c.c.}, \qquad \text{(A1)}$$

where ϕ stands for any field component, z the propagation distance, and z_0 a scale length for normalization of z. Here, we take z_0 a small value of the distance, instead of wavelength c/ω_c as given in Refs. [6,7], so as to make the quantity z/z_0 a large value for our experimental condition. The exponent $P(\omega)$ is given by

$$P(\omega) = i\frac{n\omega}{c} z_0 - i\frac{z_0}{z}\omega t + \frac{z_0}{z} \ln A(\omega), \qquad \text{(A2)}$$

where $A(\omega)$ is the Fourier amplitude of the wave packet. Using the saddle-point method, we have the asymptotic form of ϕ

$$\phi(z,t) = \sum_{\omega_s} \frac{1}{\sqrt{-\frac{z}{z_0}\left(\frac{\partial^2 P}{\partial \omega^2}\right)_{\omega_s}}} \exp\left[\frac{z}{z_0} P(\omega_s)\right] + \text{c.c.}, \qquad \text{(A3)}$$

where the saddle point ω_s is determined by $\partial P/\partial\omega = 0$, and is a function of both z and t.

For a Gaussian-modulated pulse with a central wave frequency ω_c and a pulse width Δ, the Fourier amplitude is given by

$$A(\omega) = \Delta \exp\left[-\Delta^2 \frac{(\omega - \omega_c)^2}{2}\right], \qquad \text{(A4)}$$

and the saddle point ω_s is determined by

$$\left(\frac{\partial P}{\partial \omega}\right)_{\omega_s} = i\frac{z_0}{c}\left[\left(\frac{\partial n\omega}{\partial \omega}\right)_{\omega_s} - \frac{ct}{z}\right] - \frac{z_0}{z}\Delta^2(\omega_s - \omega_c) = 0. \tag{A5}$$

At a certain propagation distance, the peak position of the envelope, which is determined by $\mathrm{Re}[\partial P(\omega_s(t),t)/\partial t] = 0$, is equivalent to

$$\mathrm{Im}[\omega_s] = 0. \tag{A6}$$

Namely, the saddle point corresponding to the maximum of the amplitude locates on the real axis and we thus put $\omega_s = \omega_1$ (real number) for the peak position. Substituting ω_1 into Eq. (A5) and separating it into real and imaginary parts, we obtain

$$\frac{z}{ct} = \frac{1}{\mathrm{Re}\left(\dfrac{\partial n\omega}{\partial \omega}\right)_{\omega_1}}, \tag{A7}$$

$$\omega_1 - \omega_c = -\frac{z}{c\Delta^2}\mathrm{Im}\left(\frac{\partial n\omega}{\partial \omega}\right)_{\omega_1}. \tag{A8}$$

Equation (A7) is the average propagation velocity normalized by the light velocity and Eq. (A8) is the central frequency shift at a given distance z. When the imaginary part of the refractive index in Eq. (A8) is negligibly small, ω_1 reduces to ω_c, and Eq. (A7) is hence identical with the conventional group velocity given by Eq. (1).

[1] L. Brillouin, *Wave Propagation and Group Velocity* (Academic, New York, 1960).
[2] C. G. B. Garrett and D. E. McCumber, Phys. Rev. A **1**, 305 (1970).
[3] M. D. Crisp, Phys. Rev. A **4**, 2104 (1971).
[4] K. Suchy, J. Plasma Phys. **8**, 33 (1972).
[5] E. L. Bolda, R. Y. Chiao, and J. C. Garrison, Phys. Rev. A **48**, 3890 (1993).
[6] M. Tanaka, M. Fujiwara, and H. Ikegami, Phys. Rev. A **34**, 4851 (1986).
[7] M. Tanaka, Plasma Phys. Contr. Fusion **31**, 1049 (1989).
[8] L. Muschietti and C. T. Dum, Phys. Fluids B **5**, 1383 (1993).
[9] Y. Amagishi and M. Tanaka, Phys. Rev. Lett. **71**, 360 (1993).
[10] Y. Amagishi and A. Tsushima, Plasma Phys. Contr. Fusion **26**, 1489 (1984).
[11] Y. Amagishi, Phys. Rev. Lett. **57**, 2807 (1986).
[12] Y. Amagishi, K. Saeki, and I. J. Donnelly, Plasma Phys. Contr. Fusion **31**, 675 (1989).
[13] Y. Amagishi, Phys. Rev. Lett. **64**, 1247 (1990).